Electronic structure of the trimethylenemethane diradical in its ground and electronically excited states: Bonding, equilibrium geometries, and vibrational frequencies

Lyudmila V. Slipchenko and Anna I. Krylov[a)]
Department of Chemistry, University of Southern California, Los Angeles, California 90089-0482

Accurate equilibrium properties of the ground and the three lowest excited states of the trimethylenemethane (TMM) diradical are calculated by using the novel spin–flip electronic structure method. Changes in structures and vibrational frequencies upon excitation are analyzed. The bonding picture in different states of TMM is derived from wave function analysis and comparison of equilibrium structures with typical values of coupled-cluster (CC) bond lengths, e.g., a double CC bond in ethylene, a single CC bond in twisted ethylene, and a bond in the allyl radical. © *2003 American Institute of Physics.* [DOI: 10.1063/1.1561052]

I. INTRODUCTION

Trimethylenemethane (TMM) is an example of a non-Kekulé system (see Fig. 1). The π system of TMM consists of four π electrons which can be distributed over four molecular π-type orbitals in a number of different ways (Figs. 2 and 3). The unusual electronic structure of TMM was recognized by Moffit and Coulson more than 50 years ago.[1] Two years later, in 1950, Longuet-Higgins analyzed the electronic structure of several non-Kekulé molecules, TMM included.[2] Since then, TMM has attracted avid attention of theoreticians[3–31] and experimentalists.[32–39] In addition to its fascinating electronic structure, there are other reasons for such a persistent interest. For example, TMM is an intermediate in the formation and rearrangements of methylenecyclopropanes.[40,41] Other practical applications of TMM derivatives include organic ferromagnets,[42,43] synthetic reagents,[44] and DNA cleaving agents.[45]

TMM was first isolated in a matrix in 1966 by Dowd,[32] who recorded its ESR spectrum. In 1976, the triplet multiplicity of the ground state of TMM was confirmed by the EPR experiment.[33] Dowd had also attempted to determine the singlet–triplet splitting in TMM,[34,35] which was measured later by photoelectron spectroscopy.[38] Recently, the infrared spectrum of the triplet ground state was reported.[36,37] Additional information about TMM's vibrational frequencies was derived from the photoelectron spectrum of the corresponding anion.[39]

Previous theoretical studies of TMM included investigation of the potential energy surfaces (PESs) of the two lowest singlet states by Borden and Davidson.[11] Energy profiles along the reaction coordinate of the methylenecyclopropane rearrangement which proceeds through the TMM intermediate, were also studied.[12,13] Numerous attempts were made to accurately determine the singlet–triplet splittings in the molecule.[14–30] Theoretical predictions of the vibrational frequencies of the triplet TMM were reported in Refs. 31 and 37.

The goal of this work is to quantitatively analyze the bonding in different electronic states of TMM, and to determine spectroscopic signatures of changes in bonding upon electronic excitation. Qualitatively, the electronic structure of TMM can be described by using a simple molecular orbital picture as has been done in earlier studies.[1,2] Later, these qualitative conclusions have been confirmed by *ab initio* calculations of optimized geometries of the triplet and the two lowest singlets:[11] the observed changes in bond lengths were consistent with earlier predictions. However, due to the methodological difficulties (see Sec. II A), it was not possible to calculate equilibrium geometries and harmonic frequencies with quantitative accuracy. Moreover, the cumbersome nature of the available methods discouraged researchers from studying higher excited states. Recently, a new electronic structure approach, the spin–flip (SF) method,[46–50] has been developed. The SF approach allows one to describe multireference wave functions within a single-reference formalism. By using the SF method, we calculated accurate equilibrium structures and vibrational frequencies of the ground and the three lowest excited states of TMM, and characterized higher excited states.

The structure of the paper is as follows: Section II describes methodological issues relevant to diradicals[9,51–53] and outlines the SF approach. In Sec. III, the results are presented: the analysis of TMM's excited states (Sec. III A), their geometries (Sec. III B) and frequencies (Sec. III C). Our concluding remarks are given in Sec. IV.

II. THEORETICAL METHODS AND COMPUTATIONAL DETAILS

A. Electronic structure of diradicals

Salem[51] defines diradicals as molecules with two electrons occupying two (near-)degenerate molecular orbitals. For such system, three singlet, $\{\Psi_i^s\}_{i=1}^3$, and three triplet, $\{\Psi_i^t\}_{i=1}^3$, wave functions can be composed as follows:[54]
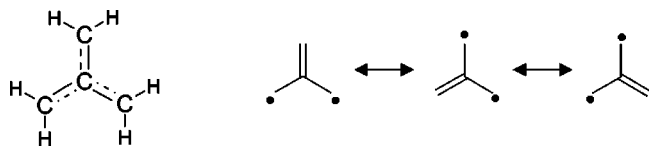
[a)]Electronic mail: krylov@usc.edu

FIG. 1. TMM (left) and its Kekulé structures (right): the π system of the molecule is fully conjugated, but each of its Kekulé structures has at least two non-π-bonded atoms.

$$\Psi_1^s = \tfrac{1}{2}[\lambda(\phi_1)^2 - \sqrt{1-\lambda^2}(\phi_2)^2] \cdot (\alpha\beta - \beta\alpha), \qquad (1)$$

$$\Psi_2^s = \tfrac{1}{2}[\sqrt{1-\lambda^2}(\phi_1)^2 + \lambda(\phi_2)^2] \cdot (\alpha\beta - \beta\alpha), \qquad (2)$$

$$\Psi_3^s = \tfrac{1}{2}(\phi_1\phi_2 + \phi_2\phi_1) \cdot (\alpha\beta - \beta\alpha), \qquad (3)$$

$$\Psi_1^t = \tfrac{1}{2}(\phi_1\phi_2 - \phi_2\phi_1) \cdot (\alpha\beta + \beta\alpha), \qquad (4)$$

$$\Psi_2^t = \frac{1}{\sqrt{2}}(\phi_1\phi_2 - \phi_2\phi_1) \cdot (\alpha\alpha), \qquad (5)$$

$$\Psi_3^t = \frac{1}{\sqrt{2}}(\phi_1\phi_2 - \phi_2\phi_1) \cdot (\beta\beta). \qquad (6)$$

Here $\phi_i\phi_j$ is a shorthand notation for the $\phi_i(1)\phi_j(2)$, and $\alpha\beta$ stands for the $\alpha(1)\beta(2)$. The coefficient λ depends on the energy gap between ϕ_1 and ϕ_2: $\lambda \approx 1$ for large energy separations (closed-shell limit), whereas for exactly degenerate orbitals $\lambda = 1/\sqrt{2}$.

From a methodological point of view, it is important that all three singlet wave functions are two-determinantal as shown in Fig. 3 (see Ref. 49 for a more detailed analysis). The open-shell singlet, Ψ_3^s, always requires two determinants, whereas the character of the closed-shell singlets, Ψ_1^s and Ψ_2^s, depends on the energy gap between the orbitals: when ϕ_1 and ϕ_2 are exactly degenerate, both closed-shell singlets consist of two equally important determinants. Therefore, the Hartree–Fock wave function, i.e., the single Slater determinant, is a qualitatively incorrect approximation for Ψ_{1-3}^s (and Ψ_1^t). Only a multiconfigurational model which treats the important determinants on an equal footing, such as multiconfigurational self-consistent field (MCSCF),[55–57] provides an appropriate zero-order wave function for a diradical.[58]

Moreover, to achieve quantitative accuracy, an appropriate zero-order wave function should be augmented by dynamical correlation, e.g., by configuration interaction[59] or perturbation theory[60–62] (see Ref. 63 for a comprehensive review of multireference methods). The inclusion of dynamical correlation is crucial for a correct quantitative (and sometimes even qualitative) description of the electronic structure of diradicals.[64–67] Bare MCSCF wave functions are known to overemphasize contributions of antibonding configurations, and therefore they systematically overestimate bond lengths and underestimate frequencies. Moreover, the stationary points of the PES corresponding to diradicals can disappear at higher level of theory.[67] That is why the common practice of optimizing geometries at the MCSCF level provides, at its best, only qualitatively correct geometries and frequencies which cannot be directly compared with experimental data. For example, in order to compare bond

lengths in TMM against reference systems (e.g., ethylene or benzene), one would have to calculate MCSCF geometries for *both* TMM *and* the reference molecules, assuming that the MCSCF errors are systematic and that changes in bond lengths will be reproduced correctly.

To summarize, the theoretical description of singlet diradicals [Eqs. (1)–(3)] is difficult due to their multireference character. The triplet diradicals' wave functions, however, are much simpler. While the $M_s=0$ triplet wave function (4) is also two-configurational, the corresponding high-spin components (5) and (6) are single-determinantal. Therefore, these states can be described by any single-reference method, the accuracy being systematically improved as one proceeds from the Hartree–Fock model toward correlated approaches. With respect to these high-spin triplet states [Eqs. (5) and (6)], all singlet states [Eqs. (1)–(3)] as well as the $M_s=0$ component of the triplet [Eq. (4)] are formally *single electron excitations involving spin–flip*. This immediately suggests that these states can be described by the appropriate single-reference based excited state theory, e.g., by configuration interaction singles (CIS),[68–70] perturbatively corrected CIS, CIS(D),[71] or equation-of-motion coupled-cluster (EOM-CC) models, e.g., EOM-CC with singles and doubles (EOM-CCSD)[72,73] or EOM optimized-orbitals coupled-cluster doubles.[74] If density functional theory (DFT) is employed to describe the reference,[75,76] the target states can be treated within the time-dependent DFT formalism.[77–79] Thus, in the spin–flip approach[46–48,50] closed and open shell singlet states are described within a single reference formalism as spin–flipping, e.g., $\alpha \rightarrow \beta$, excitations from a triplet ($M_s=1$) reference state for which both dynamical and nondynamical correlation effects are much smaller than for the corresponding singlet state. By employing theoretical models of increasing complexity for the reference wave function, the description of the final states can be systematically improved. It has been shown that the SF models describe the equilibrium properties of all three diradical states (1)–(3) and the corresponding energy separations with an accuracy comparable to that of traditional methods when applied to well-behaved molecules.[47,49,50]

B. The spin–flip method

In traditional (non-SF) single reference excited states models, the excited state wave functions are parametrized as follows:

$$\Psi_{M_s=0}^{s,t} = \hat{R}_{M_s=0}\bar{\Psi}_{M_s=0}^s, \qquad (7)$$

where $\bar{\Psi}_{M_s=0}^s$ is a closed-shell reference wave function, and the operator $\hat{R}$ is an excitation operator truncated at a certain level of excitation (which should be consistent with the theoretical model employed to describe the reference $\bar{\Psi}^s$). Note that only excitation operators which do not change the total number of α and β electrons, i.e., $M_s=0$, need to be considered in Eq. (7).

This scheme breaks down for diradicals, when the closed-shell singlet wave functions, e.g., Ψ_1^s from Eq. (1),

become multiconfigurational. To overcome this problem, the SF model employs a high-spin triplet reference state which is accurately described by a single-reference wave function. The target states, closed and open shell singlets and triplets, are described as spin–flipping excitations:

$$\Psi^{s,t}_{M_s=0} = \hat{R}_{M_s=-1}\tilde{\Psi}^{t}_{M_s=+1}, \tag{8}$$

where $\tilde{\Psi}^{t}_{M_s=+1}$ is the $\alpha\alpha$ component of the triplet reference state [Eq. (5)], $\Psi^{s,t}_{M_s=0}$ stands for the final ($M_s=0$) singlet and triplet states [Eqs. (3) and (4)], respectively, and the operator $\hat{R}_{M_s=-1}$ is an excitation operator that flips the spin of an electron. In the DFT-based variant, SF-DFT,[50] the target states are described as single electron excitations from the reference high-spin Kohn–Sham determinant.

C. Computational details

TMM's equilibrium geometries[49] and vibrational frequencies were obtained by using the SF-DFT[50,80] method with a 6-31G* basis set.[81] Additional calculations were performed by using the SF-CIS(D) and the SF-CCSD methods.[47,82] For the ground triplet state, which can be accurately described by single-reference methods, we also present results calculated by the CCSD(T) method[83] in a cc-pVTZ basis set.[84] 6-31G* and cc-pVTZ bases were used with pure angular momentum polarization functions.

The SF optimized geometries, frequencies, and total energies for the triplet state have been calculated by using the $M_s=0$ SF state rather than the $M_s=1$ reference state. In all the SF calculations, spin-unrestricted triplet references were used. All electrons were active unless specified otherwise.

All the SF calculations have been performed by using the Q-CHEM[85] *ab initio* package. The CCSD(T) results have been obtained with the ACES II electronic structure program.[86]

To streamline the discussion, C_{2v} symmetry labels are used for all the states including those whose equilibrium structures are of different symmetries, e.g., D_{3h} or C_2. The correct symmetry labels are given when needed.

III. RESULTS AND DISCUSSION

A. Low-lying excited states of TMM

The π system of TMM is presented in Fig. 2. It consists of four π electrons distributed over four molecular π-type orbitals, two of which are exactly degenerate at the D_{3h} symmetry [these are ϕ_1 and ϕ_2 from Eqs. (1) to (6)]. Therefore, in accordance with Hund's rule, the ground state of the molecule should be the $^3A_2'$ ($^3B_2$) triplet state. By rearranging two unpaired electrons in two degenerate orbitals, three different singlet states can be generated: Ψ^{s}_{1-3} from Eqs. (1)–(3), two of which (Ψ^{s}_1 and Ψ^{s}_3) being exactly degenerate at D_{3h}. These states are traditional diradical states derived from the two-electrons-in-two-orbitals model.[51] However, the electronic structure of TMM is more complicated because all four of its π orbitals are close in energy. Thus, a more appropriate description should include four electrons and four orbitals. Indeed, as we will see later, states derived
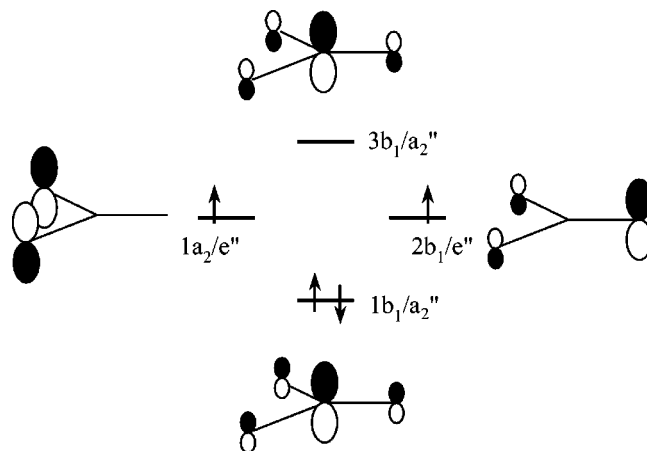

FIG. 2. The π system of TMM at the D_{3h} geometry (C_{2v} symmetry labels are also used). Due to the exact degeneracy between the two e'' orbitals at the D_{3h} structure ($1a_2$ and $2b_1$ in C_{2v} symmetry), Hund's rule predicts that the ground state of the molecule is the triplet $^3A_2'$ state ($^3B_2$ in C_{2v}).

by excitations of other π electrons within the four orbital subspace are relatively low in energy. To distinguish between different types of electronic states, we will refer to the states described by Eqs. (1)–(6) as diradical-type states.

The electronic states of TMM derived from distributing four electrons on four π orbitals are shown in Fig. 3. The vertical excitation energies used in Fig. 3 are calculated at the SF-CCSD method in a mixed basis (cc-pVTZ on carbons and cc-pVDZ on hydrogens). The first three singlet states are of a diradical type, i.e., Ψ^{s}_{1-3} from Eqs. (1) to (3). The first closed-shell $1\,^1A_1$ and the open-shell $1\,^1B_2$ singlets are exactly degenerate in D_{3h} symmetry. In accordance with the Jahn–Teller theorem,[87] the degeneracy between these singlets can be lifted at lower symmetry. The closed-shell singlet is stabilized at the planar C_{2v} geometry, with one short CC bond. The open-shell singlet prefers an equilibrium
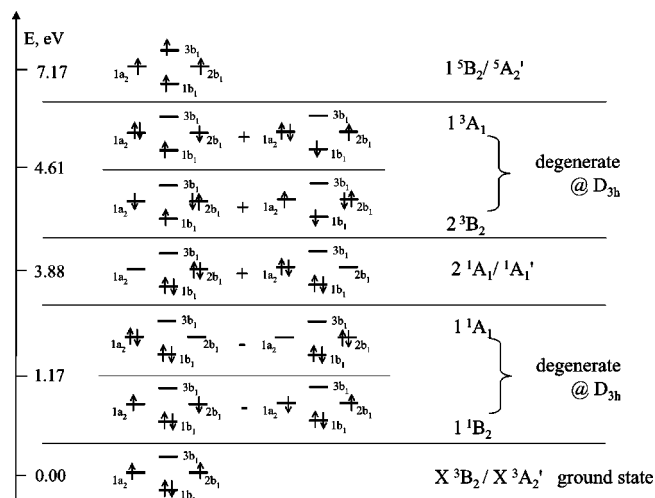

FIG. 3. Low-lying electronic states of TMM calculated at the $X\,^3A_2'$ ($^3B_2$) equilibrium geometry by the SF-CCSD method (C_{2v} labels). The degeneracy between the $1\,^1B_2/1\,^1A_1$ and the $2\,^3B_2/1\,^3A_1$ states can be lifted by lower symmetry distortions. The high-spin component of the $X\,^3B_2$ state is used as the reference in the SF calculations. The vertical excitation energies for the $1\,^3A_1$ and $2\,^3B_2$ states are obtained using the $1\,^5B_2$ reference.

structure with one long CC bond and a twisted methylene group (planar C_{2v} structure with one long CC bond corresponds to a transition state between two equivalent minima[11]). These two states have been characterized in several previous studies.[11,24,29,30] The second closed-shell singlet, $2\,^1A_1$,[14] is composed of the same determinants as the $1\,^1A_1$ state [this is the Ψ_2^s state from Eq. (2)]. Since this state prefers structures at which the diradical orbitals are exactly degenerate, its equilibrium geometry is of D_{3h} symmetry. This is similar to the $2\,^1A_1$ state of methylene and nitrenium: as explained in footnote 99 in Ref. 49, this state favors a nearly linear (CH$_2$) or linear (NH$_2^+$) structures when the $3a_1$ and $1b_1$ diradical orbitals become (nearly) degenerate. The next two states, $1\,^3A_1$ and $2\,^3B_2$, are degenerate triplets derived from excitations of one electron from the doubly occupied $1b_1$ orbital to either the a_2 or the $2b_1$ degenerate orbitals. These states can also undergo different Jahn–Teller distortions. The quintet $^5B_2$ state has all the π orbitals singly occupied and prefers D_{3h} geometry.

Note that only the $X\,^3B_2$ and $1\,^5B_2$ states can be described by a single Slater determinant. All other states from Fig. 3 are two-configurational. The traditional recipe for calculating these states would be to employ the MCSCF model (two-configurational SCF being a minimal level of theory) with the subsequent inclusion of dynamical correlation. Such calculations are usually performed in a state-by-state fashion. Moreover, even large active space MCSCF calculations would fail to reproduce the exact $1\,^1A_1/1\,^1B_2$ and $1\,^3A_1/2\,^3B_2$ degeneracies at D_{3h}, unless state averaging is performed. The SF method employs the $X\,^3B_2$ state (which also happens to be the true ground state of TMM) as the reference, and treats all other states as spin–flipping excitations. Note that the determinants employed in all the singlets and the quintet state (Fig. 3) are formally single electron excitations (with a spin–flip) from the reference high-spin triplet determinant.[88] That is why the SF approach provides a balanced description of all the singlet states of Fig. 3. For example, the exact degeneracies mentioned earlier are correctly described by any SF model. Moreover, all the states of Fig. 3 are obtained in a single SF calculation.

B. Equilibrium geometries of the $X\,^3A_2'$, $1\,^1B_1$, $1\,^1A_1$, and $2\,^1A_1$ states of TMM

Equilibrium geometries of the four lowest states of TMM are given in Ref. 49. The $X\,^3A_2'$ and $2\,^1A_1$ states have D_{3h} equilibrium geometries. The $1\,^1A_1$ state has planar C_{2v} structure with one short CC bond and two long CC bonds, whereas the $^1B_1$ state has a nonplanar structure with two short and one long CC bonds, and a twisted methylene group. At the SF-DFT/6-31G* level, the C_{2v} 90° twisted structure is a local minimum on the $^1B_1$ surface, i.e., it does not have imaginary frequencies. However, the energy of the C_2 structure with the dihedral angle of 79.0° is slightly lower in energy. We have not found any C_s minima (corresponding to the 90° twisted and pyramidazed CH$_2$ group). Overall, the potential surface along the twisting coordinate is rather flat, e.g., the energy difference between the C_{2v} (90° twisted) and the C_2 (79.0° twisted) structures is only 0.001 eV (0.03 kcal/
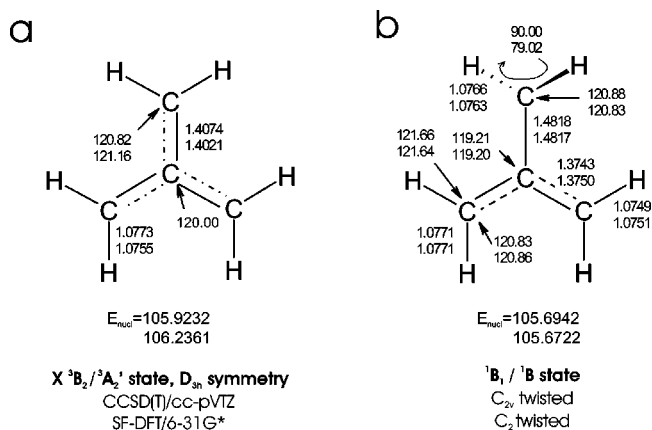

FIG. 4. (a) Geometries of the ground $^3A_2'$ state optimized at the CCSD(T)/cc-pVTZ (upper numbers) and SF-DFT/6-31G* (lower numbers) levels. (b) Geometries of the open-shell singlet optimized by the SF-DFT/6-31G* method. Upper numbers: C_{2v} twisted structure; lower numbers: C_2 twisted structure. Bond lengths are in angstroms, angles in degrees, and nuclear repulsion energies in hartrees.

mol) at the SF-DFT/6-31G* level of theory.[49] Both geometries are given in Fig. 4(b). The vibrational analysis discussed in Sec. III C confirms that the properties of both conformers are very similar.

Figure 5 compares the equilibrium structures of the molecule calculated by the SF, MCSCF, and CCSD(T) (triplet only) methods. The most interesting structural parameters are the lengths of the CC bonds since they reflect changes in π boding upon electron rearrangement. Figure 5 shows the equilibrium CC bond lengths in the ground triplet and the two lowest singlet states. At the D_{3h} symmetry, all the CC bonds are equivalent ($X\,^3A_2'/^3B_2$ and $2\,^1A_1'/^1A_1$ states). In
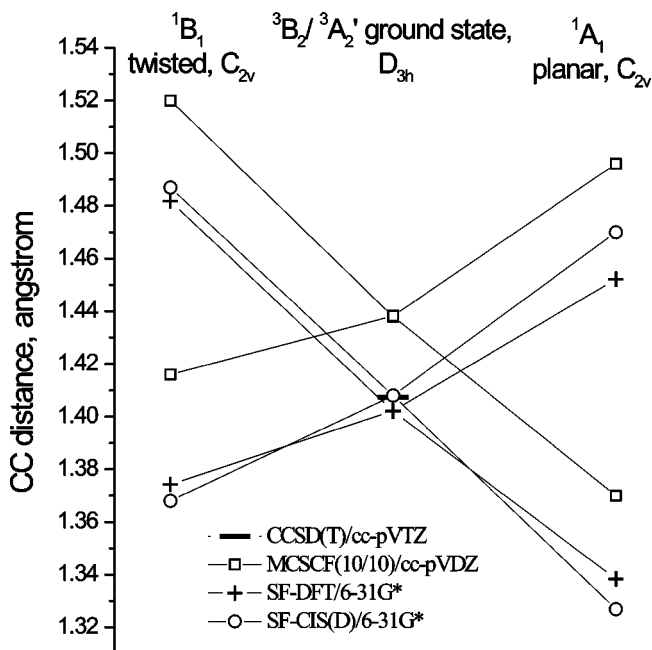

FIG. 5. The CC bond lengths in the ground triplet and the two lowest singlet states. The SF-CIS(D) and SF-DFT triplet bond lengths are very close to the CCSD(T) ones. MCSCF consistently overestimates bond lengths. State-to-state structural changes are similar in all methods.
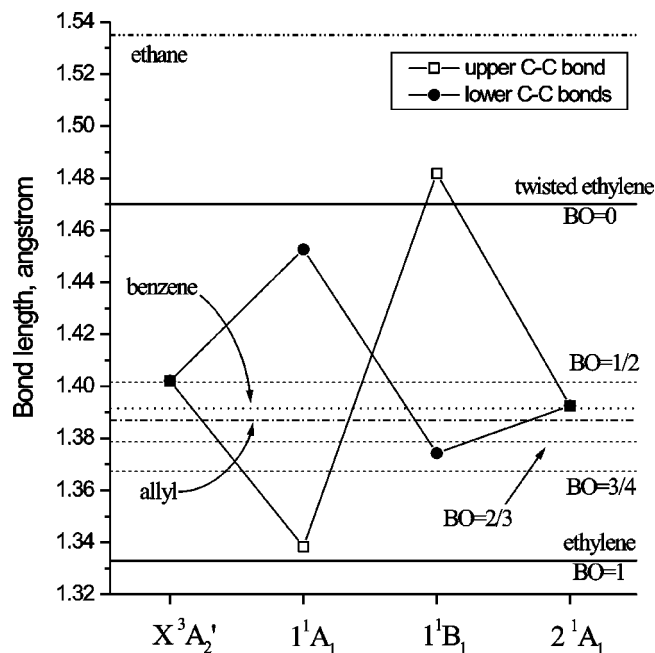
FIG. 6. The CC bond lengths in the ground and the three lowest excited states of TMM. Solid horizontal lines correspond to the values of a single (twisted ethylene) and double (ethylene) bond lengths. Dashed horizontal lines show the π-bond orders (BO) of $\frac{1}{2}$, $\frac{2}{3}$, and $\frac{3}{4}$. Ethane (dash-dot-dot line), benzene (dotted line), and allyl (dash-dot line) bonds are also shown.

the $1\,^1B_1$ state there are one long and two short bonds, whereas the $1\,^1A_1$ state has one short and two long bonds.

As shown in Fig. 5, the SF-CIS(D) and SF-DFT triplet's geometries are much closer to the (highly accurate) CCSD(T) values than the MCSCF structure with bonds that are 0.04 Å too long. The SF-DFT structures are very close to the SF-CIS(D) ones. The relative structural changes between the states are well reproduced by all the methods.

In order to understand the bonding in different electronic states of TMM, we compare the corresponding bond lengths with the typical values for single and double bonds, as in other studies establishing correlation between "bond order"-like quantities and bond lengths (see, for example, Refs. 89 and 90, and references therein). This is presented in Fig. 6. We employ the Lewis definition[91] of bond order, i.e., a number of electron pairs shared between two atoms, rather than bond orders calculated from electron density (for a brief summary of different definitions, see Ref. 89).

Our choice of reference systems has been guided by the following considerations: (i) the hybridization of the participating carbons should be the same as in TMM,[92] and (ii) the valence angles should be not strained (i.e., should be close to an optimal value for a given hybridization). Moreover, we prefer to use geometries obtained by accurate electronic structure calculations, unless anharmonicity corrections are available for the experimentally determined structures. The r_0 versus r_e difference can be much larger than the intrinsic errors of an electronic structure method. For example, in benzene, the anharmonicity corrections change the value of the CC bond from 1.391 to 1.399 Å,[93] whereas the CCSD(T)/cc-pVQZ mean absolute errors of in bond lengths are about 0.002 Å.[94]

In all four lowest states of TMM, the carbons are sp^2 hybridized and the CCC valence angles are close to $120°$. The choice of the reference double CC bond between the sp^2 hybridized carbons is straightforward: ethylene in its ground state has a full double bond and satisfies both of the above-mentioned criteria. Thus, we accept 1.333 Å[95] as the reference value for a full double bond (the π-bond order is 1). Choosing a typical single bond is more complicated. Ethane is not an appropriate candidate, because its carbons are sp^3-hybridized and, therefore, its CC bond is longer than the single bond between two sp^2 hybridized carbons.[92] A more relevant example is twisted ethylene where both carbons are sp^2 hybridized, while the π bond is broken due to the zero overlap between the p orbitals at the $90°$ twisted geometry. We accept the corresponding bond length of 1.470 Å[47] as a typical single bond value (π-bond order is 0).[96] Butadiene is another molecule with single and double bonds between sp^2 hybridized carbons. However, due to conjugation, its single bond is slightly shorter whereas the double bond is longer than in ethylene (the corresponding values are 1.467 and 1.343 Å, respectively[97]). Benzene and the allyl radical are examples of sp^2 systems with π-bond orders of $\frac{1}{2}$ and $\frac{3}{4}$, respectively. The corresponding bond lengths are 1.391 Å[93,98] and 1.387 Å.[99]

To analyze the bonding, we consider a simple model which assumes that the length of a bond with a partial π character is inversely proportional to the π-bond order. Once reference values for single and double CC bonds are agreed upon, the above-mentioned assumption enables one to calculate a π-bond order for a given bond length, or, alternatively, to estimate an expected bond length for any intermediate bond order. As can be seen from Fig. 6, the bond lengths in benzene (π-bond order of $\frac{1}{2}$) are slightly shorter than predicted by the model. Conversely, the allyl radical bonds are longer than the value obtained by assuming that all three electrons participate in two π bonds (i.e., a π-bond order of $\frac{3}{4}$). The latter discrepancy can be explained by the nearly nonbonding character of the a_2 singly occupied allyl orbital.

Assuming that the $1b_1$, $2b_1$, and $1a_2$ orbitals of TMM are of a bonding character, the π-bond order in the $^3A_2'$ and $2\,^1A_1$ states is $\frac{2}{3}$ (four π electrons equally distributed between three CC bonds). Figure 6 shows that the bond lengths in these states are slightly longer than estimated by the model. This is probably due to the nearly nonbonding character of the $2b_1$ and $1a_2$ orbitals at D_{3h} (see Fig. 2). Another interesting observation is that the bond lengths in the singlet are shorter than in the triplet. This is because electrons with parallel spins form weaker bonds due to the Pauli exclusion principle.

In the $1\,^1A_1$ state, two π electrons participate in the short (upper) bond (thus, the π character of this bond equals 1). Two other π electrons contribute to the two longer (lower) bonds, however, the resulting bonding is very weak, because of the small overlap between the two π centers. As Fig. 6 demonstrates, this picture agrees well with the actual structures: the length of the shorter bond is close to the bond in ethylene, while the longer bonds are only slightly shorter than the bond with the zero π character (e.g., twisted ethylene).

TABLE I. Vibrational frequencies, cm^{-1}, of the ground $X\,^3A_2'$ state of TMM.

	Symm	Type	Expt.[a]	Expt.[b]	CCSD(T)/cc-pVTZ[c]	SF-DFT/6-31G*[d]
ω_1/ω_2	e'	CC scissors/rock		425	427 (0.01)	440
ω_3	a_1''	H wag (OPLA)			473	485
ω_4/ω_5	e''	H wag (OPLA)			485	503
ω_6	a_2''	CC torsion (OPLA)	499.0 (0.36)		518 (0.34)	531
ω_7/ω_8	e''	H torsion (OPLA)			732	728
ω_9	a_2''	H torsion (OPLA)	755.5 (1.00)	727.5	777 (1.00)[e]	794
ω_{10}	a_1'	CC s-stretch		915	950	989
ω_{11}	a_2'	H rock			961	1002
ω_{12}/ω_{13}	e'	H-rock			1030 (<0.01)	1064
ω_{14}/ω_{15}	e'	CC a-stretch		1310	1371 (<0.01)	1416
ω_{16}/ω_{17}	e'	H scissors	1418.4 (0.15)		1518 (0.06)	1569
ω_{18}	a_1'	H scissors			1533	1593
ω_{19}/ω_{20}	e'	H s-stretch	3019–3031 (0.05)		3178 (0.10)	3283
ω_{21}	a_1'	H s-stretch			3186	3293
ω_{22}	a_2'	H a-stretch			3261	3384
ω_{23}/ω_{24}	e'	H a-stretch	3100–3115 (0.04)		3266 (0.09)	3387

[a]References 36 and 37. Intensities relative to the strongest band are given in parentheses. Additional band at 1455.6 cm^{-1} (0.05) has not been assigned.
[b]Reference 39.
[c]Calculated at the CCSD(T)/cc-pVTZ optimized geometry [see Fig. 4(a)]. IR intensities relative to the strongest band are given in parentheses.
[d]Calculated at the SF-DFT/6-31G* optimized geometry [see Fig. 4(a)].
[e]The absolute intensity is 94.30 km/mol.

The bonding in the $^1B_1$ state is more complicated. Assuming that three π electrons participate in the two shorter (lower) bonds, and one π electron contributes to the longer (upper) bond, the corresponding π-bond orders are $\frac{3}{4}$ and 0, respectively (the order of the longer bond is zero because the p orbitals of the upper and central carbons do not overlap at the twisted structure). Thus, this state is similar to the allyl radical with a twisted methylene group attached to it. However, as Fig. 6 shows, the upper bond is longer than the bond length in twisted ethylene, and the lower bonds are shorter than those in the allyl radical. This can be explained by an electron transfer from the upper to the lower part of the molecule. Indeed, according to the Mulliken and Lowdin population analysis of the electron density in $^1B_1$, the upper and central carbons are positively charged, while the lower carbons host negative charges. The degree of the charge separation can be characterized by the the permanent dipole moment which is equal 0.12 D (the dipole is directed from the upper to the lower part of the molecule). The driving force for the charge transfer is additional stabilization achieved by moving nonbonding electrons into the weakly bonding molecular orbitals of allyl. This charge transfer results in a contraction of the shorter (lower) bonds and an elongation of the longer (upper) bond.

We also performed a natural bond analysis (NBO 4.0. package[100]) to determine the bond orders in different states of TMM. However, the strongly delocalized structures with three- or four-center bonds are not well described by the NBO procedure. In a future study, we will employ an extension of NBO, natural resonance theory,[101,102] which has been developed to describe bonding in molecules with several resonance structures.

C. Harmonic vibrational frequencies of the $X\,^3A_2'$, $1\,^1B_1$, $1\,^1A_1$, and $2\,^1A_1$ states of TMM

For species with an unusual electronic structure, vibrational analysis is of particular importance, because vibrational frequencies reflect bond strengths, e.g., higher stretching frequencies correspond to stronger bonds, an increase in out-of-plane (OPLA) or torsional frequencies may be due to an increase in π-bonds' orders, etc. Thus, by comparing frequencies in different electronic states of TMM, we can learn more about bonding in these states.

Two independent experimental studies of the TMM vibrational spectrum were reported.[36,37,39] Maier and co-workers recorded gas phase IR spectra of the ground state TMM and its deuterated isotopomers.[36,37] From the vibrational structure of the photoelectron spectrum of the TMM negative ion measured by Wenthold *et al.*,[39] some vibrational frequencies for the ground $X\,^3A_2'$ triplet and the excited $1\,^1A_1$ singlet states were determined. Therefore, for the ground $X\,^3A_2'$ state of TMM, an almost complete set of the experimental vibrational frequencies is available. For the $1\,^1A_1$ state, however, only one vibrational frequency, 325 cm^{-1}, is known.[39] No frequencies for other singlets have been reported so far. Although the $1\,^1B_1$ state is adiabatically the lowest singlet state, it has not been observed in the Wenthold's experiment because of unfavorable Franck–Condon factors.

A comparison of the calculated and experimental frequencies is not straightforward due to anharmonicities.[103] Fortunately, the harmonic frequencies of the triplet state can be calculated by the highly reliable CCSD(T) method, which allows us to calibrate the SF method against CCSD(T). Table I compares the vibrational frequencies for the

TABLE II. Vibrational frequencies of the $X\,^3A_2'$, $1\,^1B_1$, $1\,^1A_1$, and $2\,^1A_1$ states of TMM, cm^{-1}.[a]

	Symm	Type	$X\,^3A_2'$	$1\,^1B_1$	$1\,^1A_1$	$2\,^1A_1$
ω_1	$a_1(e')$	CC scissors	440	477	337	510
ω_2	$b_2(e')$	CC rock	440	391	504	510
ω_3	$a_2(a_1'')$	All-H wag (OPLA)	485	649	146	112
ω_4	$a_2(e'')$	Up-H wag (OPLA)	503	330	713	454
ω_5	$b_1(e'')$	Down-H wag (OPLA)	503	601	290	454
ω_6	$b_1(a_2'')$	CC torsion (OPLA)	531	420	460	516
ω_7	$b_1(e'')$	Up-H torsion (OPLA)	728	490	951	805
ω_8	$a_2(e'')$	Down-H torsion (OPLA)	728	887	530	805
ω_9	$b_1(a_2'')$	All-H torsion (OPLA)	794	871	628	868
ω_{10}	$a_1(a_1')$	CC s-stretch	989	945	921	1019
ω_{11}	$b_2(a_2')$	All-H rock	1002	1033	994	1010
ω_{12}	$a_1(e')$	Down-H-rock	1064	1128	1082	1111
ω_{13}	$b_2(e')$	Up-H-rock	1064	1079	1207	1111
ω_{14}	$a_1(e')$	CC a/s-stretch	1416	1474	1717	1496
ω_{15}	$b_2(e')$	CC a/a-stretch	1416	1236	346	1496
ω_{16}	$a_1(e')$	Up-H scissors	1569	1639	1496	1642
ω_{17}	$b_2(e')$	Down-H scissors	1569	1570	1521	1642
ω_{18}	$a_1(a_1')$	All-H scissors	1593	1549	1571	1602
ω_{19}	$a_1(e')$	Up-H s-stretch	3283	3287	3275	3300
ω_{20}	$b_2(e')$	Down-H s-stretch	3283	3286	3288	3300
ω_{21}	$a_1(a_1')$	All-H s-stretch	3293	3297	3299	3308
ω_{22}	$b_2(a_2')$	All-H a-stretch	3384	3391	3361	3400
ω_{23}	$a_1(e')$	H a-stretch	3387	3393	3404	3403
ω_{24}	$b_2(e')$	H a-stretch	3387	3388	3402	3403

[a]All frequencies are calculated at the SF-DFT/6-31G* level at the SF-DFT optimized geometries (see Ref. 49 and Fig. 4). Symmetry labels are not applicable for the $1\,^1B_1$ state which has twisted C_2 equilibrium structure.

ground $^3A_2'$ state calculated by the SF-DFT and CCSD(T) methods with the experimental values.[36,37,39] The SF-DFT frequencies are systematically higher than the CCSD(T) ones, the average relative difference[104] being 3.1% with a standard deviation $\pm 1.1\%$, and a maximum difference of 4.3% for the ω_{11} mode.

At the D_{3h} symmetry, TMM has eight IR active vibrations (six of e' symmetry and two of a_2'' symmetry). The experimental and calculated values of the IR intensities of the active modes are also given in Table I (values in parentheses).[105] The measured IR spectrum consists of six bands (four single lines and two doublets). In Ref. 37, five of these bands are assigned as the skeleton and the hydrogen groups OPLA motions (ω_6, ω_9), the CH$_2$ scissoring mode (ω_{16}/ω_{17}), and the symmetric and asymmetric stretches in the CH$_2$ groups (ω_{19}/ω_{20} and ω_{23}/ω_{24}). This assignment is consistent both with the CCSD(T) and SF-DFT results. The 1455.6 cm^{-1} band with a relative intensity of 0.05 is interpreted as a combination vibration.[37] The normal mode analysis reveals that the following vibrations are strongly mixed: (i) the CC scissors/rock (ω_1/ω_2) and the hydrogens' rocking vibrations (ω_{12}/ω_{13}) (their sum is 1457 cm^{-1} at the CCSD(T)/cc-pVTZ level); and (ii) the skeleton asymmetric stretches (ω_{14}/ω_{15}) and the CH$_2$ scissors (ω_{16}/ω_{17}). The calculated frequencies of the latter vibrations are 1371 and 1518 cm^{-1}, respectively. Both pairs of mixed modes are IR active and can yield a band at 1455.6 cm^{-1}. Moreover, the doubled frequency of the most intense line in the spectrum, the OPLA hydrogens' deformation (ω_9), equals 1511 cm^{-1} (experimental), which is close to the frequency of the observed line. Thus, at this level of theory it is not possible to determine the nature of this band.

Four vibrational frequencies of the $X\,^3A_2'$ ground state were determined from the photoelectron experiment.[39] They were assigned as the skeleton scissoring/rocking mode (ω_1/ω_2), the hydrogens OPLA torsion motion (ω_9), and the symmetric and asymmetric carbon skeleton stretches (ω_{10} and ω_{14}/ω_{15}). These vibrations are active in the photoelectron spectrum, because they correspond to coordinates that connect the C_{2v} geometry of the anion with the D_{3h} structure of the $X\,^3A_2'$ state of the neutral TMM.

Table II presents the frequencies of the four lowest states of TMM. The frequencies for the $1\,^1B_1$ state are calculated at the lowest minimum of this state (C_2 structure), therefore, the symmetry labels for the vibrational modes are only approximate.[106] Significant changes in the skeleton frequencies and in the OPLA hydrogen group vibrations reflect structural differences between the ground state and the first two excited singlets, $1\,^1A_1$ and $1\,^1B_1$ (see Sec. III B). The rest of this section explains the observed changes in the calculated frequencies in terms of structural changes.[107]

The frequencies of the CC rock (ω_2), the wag, and OPLA torsional motions of the upper CH$_2$ group (ω_4 and ω_7) increase in the $1\,^1A_1$ state and decrease in the $^1B_1$ state (as compared with the $X\,^3A_2'$ triplet state). This is because these modes involve vibration of the upper CC bond, which becomes stronger and shorter in the closed-shell singlet, and is weaker in the open-shell singlet. Conversely, vibrations involving the lower carbons [i.e., the CC scissoring mode (ω_1), the wagging, and OPLA motions of the lower CH$_2$ groups ($\omega_3, \omega_5, \omega_9$, and ω_8)], have higher frequencies in the $1\,^1B_1$ state and lower frequencies in the $1\,^1A_1$ state.

Analysis of the vibrational modes that involve both the

upper and the lower parts of the molecule is more complicated. The molecule becomes softer with respect to the OPLA distortions, because the π system is disturbed at the C_{2v} structures (as compared with the D_{3h} structure of the ground state). This results in decrease of the OPLA carbon frequency (ω_6) in both the open- and closed-shell singlets. The decrease in ω_6 is larger for the open-shell C_2 structure with one p orbital having zero overlap with the other p orbitals. The frequency of the symmetric skeleton stretching mode (ω_{10}) is lower in both singlet states because the molecular skeleton is less rigid in these states with respect to the triplet state. This is consistent with the following structural changes (see also Sec. III B). The sum of the CC bond lengths increases in the following sequence: $X\,^3A_2'$, $1\,^1B_1$, and $1\,^1A_1$ state (the values are 4.206, 4.231, and 4.244 Å, respectively). Degeneracy between two asymmetric skeleton stretches at the D_{3h} symmetry is lifted at equilibrium geometries of both lowest singlets. The frequency of the a_1 vibration (ω_{14}), which is dominated by the out-of-phase vibration of the upper and two lower CC bonds, increases. The b_2 vibration (ω_{15}) (the out-of-phase vibration of the lower CC bonds, with the upper CC bond being frozen) becomes softer. In both cases, the difference is larger for the $1\,^1A_1$ state for which the b_2 asymmetric stretch frequency equals $346\,\text{cm}^{-1}$. We find that these modes are strongly mixed with the carbon scissoring and rocking vibrations and with the rocking motions of the CH_2 groups.

The second closed-shell singlet, $2\,^1A_1$, has D_{3h} equilibrium structure with the CC bond lengths slightly shorter than in the ground state (see Sec. III B). Consequently, the frequencies of the skeleton and hydrogen in-plane modes are higher in the $2\,^1A_1$ state. However, the carbon OPLA vibrations and the wagging motions of the hydrogens are lower in the singlet state. The frequencies of the latter modes are related to the stability of the molecule with respect to the rearrangement from a diradical to a methylenecyclopropane structure. Relative to the triplet state, all three singlets have lower frequencies of the hydrogens wagging modes, which suggests that these states have lower barriers for such rearrangements. Moreover, the skeleton asymmetric stretch (ω_{15}), a mode that connects open- and closed-shell singlet structures, has lower frequencies in both the $1\,^1B_1$ and $1\,^1A_1$ states than in the triplet state.

From the vibrational structure of the photoelectron spectrum, Wenthold et al.[38,39] have determined one frequency of $325\,\text{cm}^{-1}$ for the $1\,^1A_1$ state. Our calculated harmonic frequencies suggest that the observed $325\,\text{cm}^{-1}$ mode can be assigned to either the CC scissoring ($\omega_1 = 337\,\text{cm}^{-1}$) or the CC asymmetric stretching ($\omega_{15} = 346\,\text{cm}^{-1}$) mode. Both vibrations are active in the ground triplet state in the photoelectron spectrum.

IV. CONCLUSIONS

The SF method accurately describes diradicals within a single-reference formalism. The SF-DFT method is applied to the low-lying excited states of TMM. In addition to the previous benchmarks,[47,49,50] we show that the SF-DFT triplet equilibrium properties are very close to the CCSD(T)/cc-

pVTZ results. For example, the difference in the CC bond lengths is about 0.005 Å, and the average relative differences in the harmonic frequencies are about 3%. Since the SF model treats all diradical states in a uniform fashion, we expect that the SF-DFT equilibrium structures and vibrational frequencies of all four lowest states of TMM to be of the similar accuracy. Using these structures and frequencies, we also analyze the bonding in the TMM ground and the lowest excited states. We find that the $1\,^1A_1$ state has a full double bond between the central and one of the peripheral carbons, while there is only very little interaction between two other carbons that host unpaired electrons. Although the $1\,^1B_1$ state is similar to the allyl radical with a twisted methylene group, the corresponding CC bonds in TMM are shorter than those in allyl because of electron transfer from the twisted methylene to the allyl moiety. The excited $2\,^1A_1$ state has stronger bonds relative to the ground $X\,^3A_2'$ state. Otherwise, these two states are very similar, i.e., both have D_{3h} equilibrium structures. Overall, our results demonstrate that the SF method is a useful tool for studying diradicals.

[1] C. A. Coulson, J. Chim. Phys. Phys.-Chim. Biol. **45**, 243 (1948).
[2] H. C. Longuet-Higgins, J. Chem. Phys. **18**, 265 (1950).
[3] F. Weiss, Q. Rev., Chem. Soc. **24**, 278 (1970).
[4] P. Dowd, Acc. Chem. Res. **5**, 242 (1972).
[5] W. T. Borden and E. R. Davidson, J. Am. Chem. Soc. **99**, 4587 (1977).
[6] J. A. Berson, Acc. Chem. Res. **11**, 446 (1978).
[7] A. A. Ovchinnikov, Theor. Chim. Acta **47**, 297 (1978).
[8] W. T. Borden and E. R. Davidson, Acc. Chem. Res. **14**, 69 (1981).
[9] Diradicals, edited by W. T. Borden (Wiley, New York, 1982).
[10] W. T. Borden, H. Iwamura, and J. A. Berson, Acc. Chem. Res. **27**, 109 (1994).
[11] E. R. Davidson and W. T. Borden, J. Am. Chem. Soc. **99**, 2053 (1977).
[12] D. Feller, K. Tanaka, E. R. Davidson, and W. T. Borden, J. Am. Chem. Soc. **104**, 967 (1982).
[13] S. B. Lewis, D. A. Hrovat, S. J. Getty, and W. T. Borden, J. Chem. Soc., Perkin Trans. 2 **2**, 2339 (1999).
[14] D. R. Yarkony and H. F. Schaefer III, J. Am. Chem. Soc. **96**, 3754 (1974).
[15] W. J. Hehre, L. Salem, and M. R. Willcott, J. Am. Chem. Soc. **96**, 4328 (1974).
[16] J. H. Davis and W. A. Goddard, J. Am. Chem. Soc. **99**, 4242 (1977).
[17] D. M. Hood, H. F. Schaefer III, and R. M. Pitzer, J. Am. Chem. Soc. **100**, 2227 (1978).
[18] D. M. Hood, H. F. Schaefer III, and R. M. Pitzer, J. Am. Chem. Soc. **100**, 8009 (1978).
[19] D. A. Dixon, R. Foster, T. A. Halgren, and W. N. Lipscomb, J. Am. Chem. Soc. **100**, 1359 (1978).
[20] D. Feller, W. T. Borden, and E. R. Davidson, J. Chem. Phys. **74**, 2256 (1981).
[21] S. B. Auster, R. M. Pitzer, and M. S. Platz, J. Am. Chem. Soc. **104**, 3812 (1982).
[22] W. T. Borden, E. R. Davidson, and D. Feller, Tetrahedron **38**, 737 (1982).
[23] P. M. Lahti, A. R. Rossi, and J. A. Berson, J. Am. Chem. Soc. **107**, 2273 (1985).
[24] A. Skanche, L. J. Schaad, and B. A. Hess, Jr., J. Am. Chem. Soc. **110**, 5315 (1988).
[25] S. Olivella and J. Salvador, Int. J. Quantum Chem. **37**, 713 (1990).
[26] T. P. Radhakrishnan, Tetrahedron Lett. **32**, 4601 (1991).

[27] A. S. Ichimura, N. Koga, and H. Iwamura, J. Phys. Org. Chem. **7**, 207 (1994).

[28] W. T. Borden, Mol. Cryst. Liq. Cryst. **232**, 195 (1993).

[29] C. J. Cramer and B. A. Smith, J. Phys. Chem. **100**, 9664 (1996).

[30] B. Ma and H. F. Schaefer III, Chem. Phys. **207**, 31 (1996).

[31] C. P. Blahous III, Y. Xie, and H. F. Schaefer III, J. Chem. Phys. **92**, 1174 (1990).

[32] P. Dowd, J. Am. Chem. Soc. **88**, 2587 (1966).

[33] R. J. Baseman, D. W. Pratt, M. Chow, and P. Dowd, J. Am. Chem. Soc. **98**, 5726 (1976).

[34] P. Dowd and M. Chow, J. Am. Chem. Soc. **99**, 6438 (1977).

[35] P. Dowd and M. Chow, Tetrahedron **38**, 799 (1982).

[36] G. Maier, H. P. Reisenauer, K. Lanz, R. Tross, D. Jurgen, B. A. Hess, Jr., and L. D. Schaad, Angew. Chem. Int. Ed. Engl. **32**, 74 (1993).

[37] G. Maier, D. Järgen, R. Tross, H. P. Reisenauer, B. A. Hess, Jr., and L. J. Schaad, Chem. Phys. **189**, 383 (1994).

[38] P. G. Wenthold, J. Hu, R. R. Squires, and W. C. Lineberger, J. Am. Chem. Soc. **118**, 475 (1996).

[39] P. G. Wenthold, J. Hu, R. R. Squires, and W. C. Lineberger, J. Am. Soc. Mass Spectrom. **10**, 800 (1999).

[40] W. V. E. Doering and H. D. Roth, Tetrahedron **26**, 2825 (1970).

[41] J. J. Gajewski, *Hydrocarbon Thermal Isomerizations* (Academic, New York, 1981).

[42] D. Dougherty, Acc. Chem. Res. **24**, 88 (1991).

[43] S. J. Jacobs, D. A. Shultz, R. Jain, J. Novak, and D. A. Dougherty, J. Am. Chem. Soc. **115**, 1744 (1993).

[44] B. M. Trost, Angew. Chem. Int. Ed. Engl. **25**, 1 (1986).

[45] T. M. Bregant, J. Groppe, and R. D. Little, J. Am. Chem. Soc. **116**, 3635 (1994).

[46] A. I. Krylov, Chem. Phys. Lett. **338**, 375 (2001).

[47] A. I. Krylov and C. D. Sherrill, J. Chem. Phys. **116**, 3194 (2002).

[48] A. I. Krylov, Chem. Phys. Lett. **350**, 522 (2001).

[49] L. V. Slipchenko and A. I. Krylov, J. Chem. Phys. **117**, 4694 (2002).

[50] Y. Shao, M. Head-Gordon, and A. I. Krylov, J. Chem. Phys. **118**, 4807 (2003).

[51] L. Salem and C. Rowland, Angew. Chem. Int. Ed. Engl. **11**, 92 (1972).

[52] V. Bonačić-Koutecký, J. Koutecký, and J. Michl, Angew. Chem. Int. Ed. Engl. **26**, 170 (1987).

[53] J. Michl, J. Mol. Struct.: THEOCHEM **260**, 299 (1992).

[54] Note that due to the Pauli principle the spatial parts of singlets are symmetric with respect to the interchange of two electrons, whereas the spatial parts of triplets are antisymmetric. This causes all the two-electron triplet states to be purely covalent. The physical explanation of this formal result is that the Pauli principle does not allow two electrons with the same spin to coexist in the same volume of space, as required in ionic (or zwitter-ionic) configurations. The character of the singlet states depend on the nature of the orbitals, and can vary from purely ionic to purely covalent wave functions. A detailed analysis of the diradical wave functions can be found in Refs. 9, 49, 51–53.

[55] B. O. Roos, P. R. Taylor, and P. E. M. Siegbahn, Chem. Phys. **48**, 157 (1980).

[56] K. Ruedenberg, M. W. Schmidt, M. M. Gilbert, and S. T. Elbert, Chem. Phys. **71**, 41 (1982).

[57] M. W. Schmidt and M. S. Gordon, Annu. Rev. Phys. Chem. **49**, 233 (1998).

[58] More rigorously, even MCSCF is not an ideal zero-order wave function. For example, it fails to reproduce the degeneracy between closed and open shell singlets in cases when ϕ_1 and ϕ_2 are exactly degenerate (as it happens in linear methylene or in D_{3h} TMM), unless state-averaged orbital optimization is performed.

[59] See articles by B. O. Roos; P. Bruna and S. D. Peyerimhoff; R. Shepard; and D. L. Cooper, J. Gerratt, and M. Raimondi, in *Ab Initio Methods in Quantum Chemistry, II* (Wiley, New York, 1987).

[60] K. Andersson, P.-Å. Malmqvist, B. O. Roos, A. J. Sadlej, and K. Wolinski, J. Phys. Chem. **94**, 5483 (1990).

[61] K. Andersson, P.-Å. Malmqvist, and B. O. Roos, J. Chem. Phys. **96**, 1218 (1992).

[62] H. Nakano, J. Chem. Phys. **99**, 7983 (1993).

[63] *Recent Advances in Multireference Methods*, edited by K. Hirao (World Scientific, Singapore, 1999).

[64] E. R. Davidson, J. Phys. Chem. **100**, 6161 (1996).

[65] P. M. Kozlowski, M. Dupuis, and E. R. Davidson, J. Am. Chem. Soc. **117**, 774 (1995).

[66] W. T. Borden and E. R. Davidson, Acc. Chem. Res. **29**, 67 (1996).

[67] N. W. Moriarty, R. Lindh, and G. Karlsröm, Chem. Phys. Lett. **289**, 442 (1998).

[68] I. Tamm, J. Phys. (Moscow) **9**, 449 (1945).

[69] J. A. Pople, Trans. Faraday Soc. **49**, 1375 (1953).

[70] J. B. Foresman, M. Head-Gordon, J. A. Pople, and M. J. Frisch, J. Phys. Chem. **96**, 135 (1992).

[71] M. Head-Gordon, R. J. Rico, M. Oumi, and T. J. Lee, Chem. Phys. Lett. **219**, 21 (1994).

[72] H. Koch, H. J. Aa. Jensen, and P. Jørgensen, J. Chem. Phys. **93**, 3345 (1990).

[73] J. F. Stanton and R. J. Bartlett, J. Chem. Phys. **98**, 7029 (1993).

[74] A. I. Krylov, C. D. Sherrill, and M. Head-Gordon, J. Chem. Phys. **113**, 6509 (2000).

[75] P. Hohenberg and W. Kohn, Phys. Rev. **136**, B864 (1964).

[76] W. Kohn and L. J. Sham, Phys. Rev. **140**, A1133 (1965).

[77] E. Runge and E. K. U. Gross, Phys. Rev. Lett. **52**, 997 (1984).

[78] R. Bauernschmitt and R. Ahlrichs, Chem. Phys. Lett. **256**, 454 (1996).

[79] S. Hirata and M. Head-Gordon, Chem. Phys. Lett. **314**, 291 (1999).

[80] We used the functional composed of the equal mixture of the following exchange and correlation parts: 50% Hartree–Fock+8% Slater+42% Becke for exchange, and 19% VWN+81% LYP for correlation.

[81] P. C. Hariharan and J. A. Pople, Theor. Chim. Acta **28**, 213 (1973).

[82] S. V. Levchenko and A. I. Krylov (unpublished).

[83] P. Piecuch, S. A. Kucharski, and R. J. Bartlett, J. Chem. Phys. **110**, 6103 (1999).

[84] T. H. Dunning, Jr., J. Chem. Phys. **90**, 1007 (1989).

[85] J. Kong, C. A. White, A. I. Krylov *et al.*, J. Comput. Chem. **21**, 1532 (2000).

[86] J. F. Stanton, J. Gauss, J. D. Watts, W. J. Lauderdale, and R. J. Bartlett, ACES II, 1993. The package also contains modified versions of the MOLECULE Gaussian integral program of J. Almlöf and P. R. Taylor, the ABACUS integral derivative program written by T. U. Helgaker, H. J. Aa. Jensen, P. Jørgensen, and P. R. Taylor, and the PROPS property evaluation integral code of P. R. Taylor.

[87] H. A. Jahn and E. Teller, Proc. R. Soc. London, Ser. A **161**, 220 (1937).

[88] Unlike the singlet states, the SF description of the $1\,^3A_1$ and $2\,^3B_2$ states is not perfectly balanced: while one of the configurations in both triplets is a single electron excitation from the $X\,^3B_2$ reference, the second is formally a double excitation. Moreover, both states are strongly mixed with two higher triplet configurations: $1b_1^2 2b_1 3b_1$ and $1b_1^2 2a_1 3b_1$. This imbalance results in a considerable spin contamination of the $1\,^3A_1$ and $2\,^3B_2$ states. However, the exact degeneracy between the states is preserved. Much better description of these triplets can be achieved in the SF calculation by using the quintet reference, i.e., a high-spin ($M_s=2$) component of the $^5B_2$ state. Note that from this reference, the high-spin ($M_s=1$) components of all the triplets (i.e., the ground $^3A_2'$ state, the $1\,^3A_1$, and $2\,^3B_2$ triplets) are single spin–flipping excitations. At the SF-CCSD level in a mixed basis set (cc-pVTZ on carbon and cc-pVDZ on hydrogen), the vertical energy gaps between the $X\,^3B_2$ and $1\,^3A_1/2\,^3B_2$ states calculated from the triplet and quintet references are 6.005 and 4.610 eV, respectively.

[89] E. D. Glendening, J. K. Badenhoop, and F. Weinhold, J. Comput. Chem. **19**, 610 (1998).

[90] E. D. Glendening, J. K. Badenhoop, and F. Weinhold, J. Comput. Chem. **19**, 628 (1998).

[91] G. N. Lewis, *Valence and the Structure of Atoms and Molecules* (The Chemical Catalog Company, New York, 1923).

[92] The length of a carbon–carbon *single* bond depends strongly on the hybridization of participating atoms [M. J. S. Dewar and H. N. Schmeising, Tetrahedron **5**, 166 (1959)]: the increase in the *s*-character causes bond contraction. Thus, the *single* bond length between two sp^x–sp^y hybridized centers increases in the following order: sp^2–sp^2, sp^2–sp^3, sp^3–sp^3. Of course, when *p* electrons from sp^2-hybridized atoms are available for bonding, the bond order increases due to π bonding, and the bond contracts further.

[93] J. Gauss and J. F. Stanton, J. Phys. Chem. A **104**, 2865 (2000).

[94] T. Helgaker, P. Jørgensen, and J. Olsen, *Molecular Electronic Structure Theory* (Wiley, New York, 2000).

[95] The equilibrium structure of ethylene is calculated at the CCSD(T)/cc-pVTZ level. The experimental CC bond in ethylene equals 1.339 Å (Ref. 107). The discrepancy is much larger than the method's intrinsic error of about 0.002 Å and is due to anharmonicity.

[96] This value is surprisingly close to 1.479 Å suggested by Dewar and Schmeising in 1960 as a typical value of a single bond between sp^2 hybridized carbons [M. J. S. Dewar and H. N. Schmeising, Tetrahedron **11**, 96 (1960)].

[97] W. Haugen and M. Traetteberg, Int. J. Syst. Autom.: Res. Appl. **20**, 1726 (1966).

[98] Again, as in case of ethylene, the experimental (1.399 Å, Ref. 107) and high level theoretical (1.391 Å, Ref. 103) CC bond lengths are very different due to anharmonicities.

[99] E. Hirota, C. Yamada, and M. Okunishi, J. Chem. Phys. **97**, 2963 (1992).

[100] E. D. Glendening, J. K. Badenhoop, A. E. Reed, J. E. Carpenter, and F. Weinhold, NBO 4.0, Theoretical Chemistry Institute, University of Wisconsin, Madison, WI, 1996.

[101] F. Weinhold and C. R. Landis, Chem. Ed.: Res. Pract. Eur. **2**, 91 (2001).

[102] E. D. Glendening, J. K. Badenhoop, A. E. Reed, J. E. Carpenter, J. A. Bohmann, C. M. Morales, and F. Weinhold, NBO 5.0 Program, Theoretical Chemistry Institute, University of Wisconsin, Madison, WI, 2001.

[103] The experimentally measured frequencies are the fundamentals, i.e., the energy differences between the zero and first vibrational levels. The calculated harmonic frequencies are equal to the fundamentals only for pure harmonic potentials. For a real anharmonic potential, the fundamentals can be lower (this is often a case for stretching vibrations) or higher (as can happen for OPLA modes) than the harmonic frequencies. Moreover, anharmonic terms can couple harmonic vibrational modes, which can strongly affect the observed intensities, e.g., some frequencies may not be observed due to anharmonicities.

[104] The relative differences between the SF-DFT and CCSD(T) frequencies are calculated as $(\omega_{i,\text{CCSD(T)}} - \omega_{i,\text{SF-DFT}})/\omega_{i,\text{CCSD(T)}} \times 100\%$.

[105] The SF-DFT IR intensities are not available because the analytic gradients for this method have not yet been implemented.

[106] The vibrational analysis shows that the C_2 and C_{2v} twisted structures are very similar. The largest change is in the frequency corresponding to the rotation of the upper CH_2 group (H-wag, ω_4): in C_{2v} twisted structures this frequency is 187 cm^{-1} (versus 330 cm^{-1} in C_2). Changes in other frequencies do not exceed 15 cm^{-1}.

[107] G. Herzberg, *Molecular Spectroscopy and Molecular Structure: Electronic Spectra and Electronic Structure of Polyatomic Molecules, Volume III* (van Nostrand Reinhold, New York, 1966).